Mid-Infrared Laser Development for High Intensity Experiments

IMPERIAL

AFOSR Award No. FA9550-16-1-0013
EPSRC EP/N018680/1

Annabel E Gunn*, Nicholas H Stuart, Jack Morse, Stuart P D Mangles, Roland A Smith
Blackett Laboratory, Imperial College London, South Kensington Campus, London SW7 2AZ, UK. *a.gunn21@imperial.ac.uk

CHIMERA

The Chimera Laser System.

The Chimera laser system is a custom built, high intensity, multi-beam (3.7 µm, 1.5 µm & 0.8 µm) OPCPA system currently under active development at Imperial College London, co-funded by DSTL, EPSRC and AFOSR. It's primary goal is to produce an ultra-short, high intensity pulse (< 30 fs, 25 mJ) in the mid-infrared (MIR) spectral range (3.7 µm) with a high enough intensity to drive routine high harmonic genration (HHG) and laser wakefield acceleration (LWFA) experiments - the motivation for this being primarly the attractive wavelength scaling to poderamotive energy, $U_p \propto I\lambda^2$. It is a highly complex system, containing both classical storage gain amplifcation as well as a cascade of 9 nonlinear stages. Although there are several MIR systems in development worldwide [1-3], only one such system currently shares our MIR capability [4]. Here we present our premilinary HHG results as well as particle-in-cell simulations, which will be used to plan a LWFA experiment with our MIR beam.

1. The Femtolasers Rainbow Oscillator.

All wavelengths of the OPCPA Chimera laser system originate from a single master oscillator, centred at 800 nm, meaning that both signal and pump lines are seeded from a single source. This avoids the need for external electronic synchronisation or indeed a second oscillator. It also contains the capability for carrier envelope phase (CEP) control, something which could be of great importance when aiming to deliver few-cycle, high-intensity light into an experiment.

Stable and consistent oscillator performance is essential. Power then, is the most obvious thing to monitor. Whilst increasing the pump power of the laser increases modelocked power, stability, and spectral bandwidth, it also reduces over all efficiency as well as impacting the lifetime of the system.

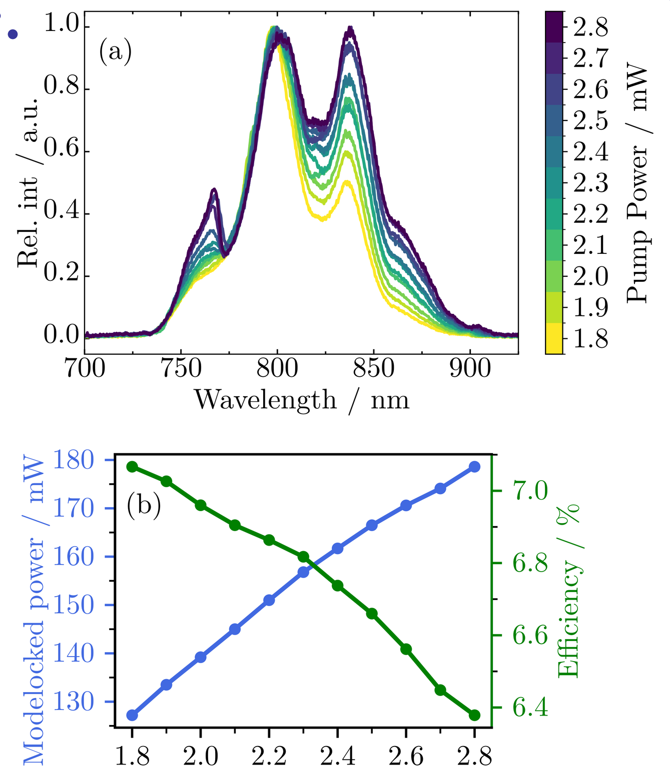

Figure 1: (a) Oscillator spectra at increasing pump powers (1.8 mW - 2.8 mW).
(b) Modelocked power and conversion efficiency for increasing pump powers (1.8 mW - 2.8 mW). We see a marked decrease in conversion efficiency for increasing pump powers.

3. MIR Generation and HHG Proof of Principle.

To generate our initial MIR pulse, we use a difference frequency generation (DFG) process, seeded by a small 800 nm OPCPA sub-system directed into a periodically poled lithium niobate (PPLN) crystal. This produces a 3.7 µm central bandwidth pulse with ~1 µm of bandwidth. To amplify the MIR, we use optical parametric amplification using potassium titanyle arsenate (KTA), with a 1053 nm pump.

Figure 4 shows the first results of our 3.7 µm pulse, picked off after the first MIR OPA (before compression), driving a HHG experiment. With a ZnSe sample, we see up to the 8th harmonic.

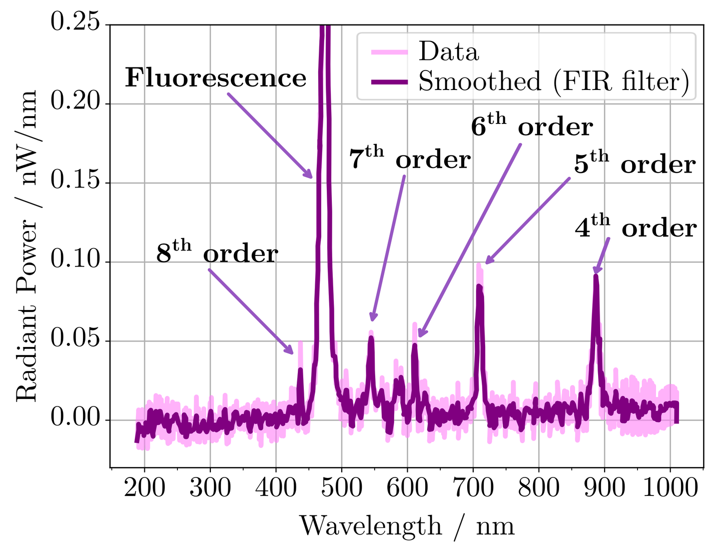

Figure 4: High harmonic spectral data obtained when directing a 1 µm bandwidth 3.7 µm pulse at a sample of ZnSn. We see up to the 8th order harmonic.

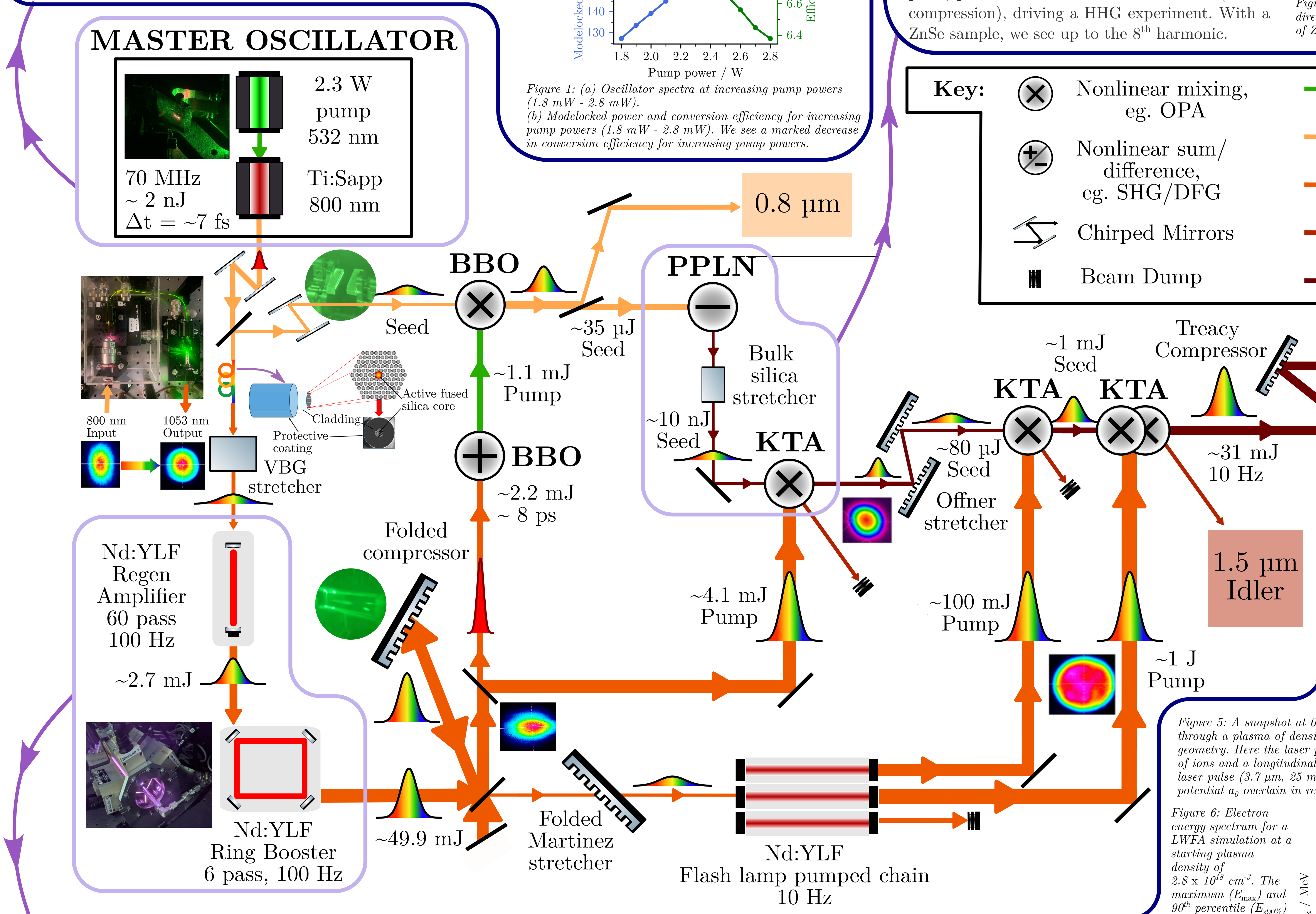

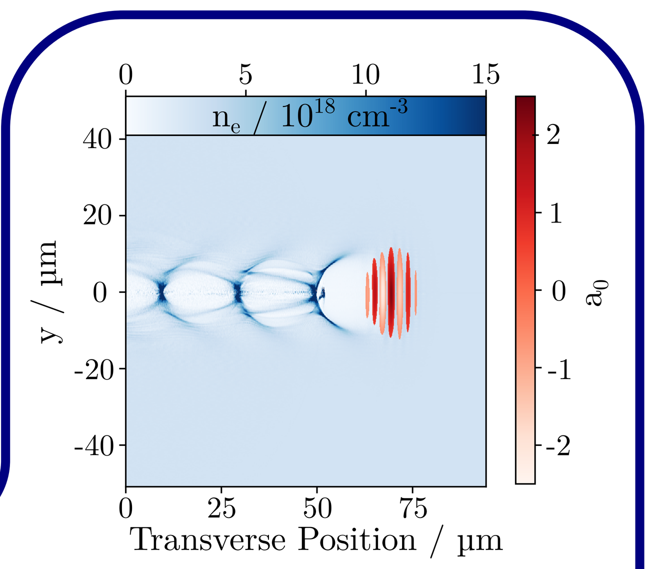

Figure 5: A snapshot at 0.80 ps of the interaction of the Chimera laser through a plasma of density of 2.8 x 10^18 cm^-3 in AM cylindrical (quasi-3D) geometry. Here the laser pulse travels from left to right, creating a channel of ions and a longitudinal oscillation of elections in its wake. The driving laser pulse (3.7 µm, 25 mJ, 30 fs) is identified by its normalised vector potential a_0 overlain in red.

Figure 6: Electron energy spectrum for a LWFA simulation at a starting plasma density of 2.8 x 10^18 cm^-3. The maximum (E_{max}) and 90th percentile ($E_{x90\%}$) electron energies E_x of distributed charge are extracted and overlaid onto the waterfall plot.

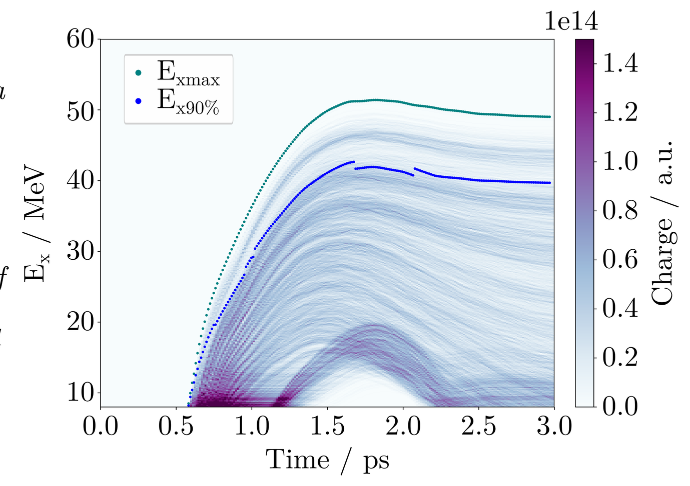

2. The Regen & Ring Storage-Gain Amplifiers.

Two 'standard' storage-gain amplifiers in use are 100 Hz diode pumped Nd:YLF laser heads used within optically switched cavities to amplify propagating 1053 nm light.

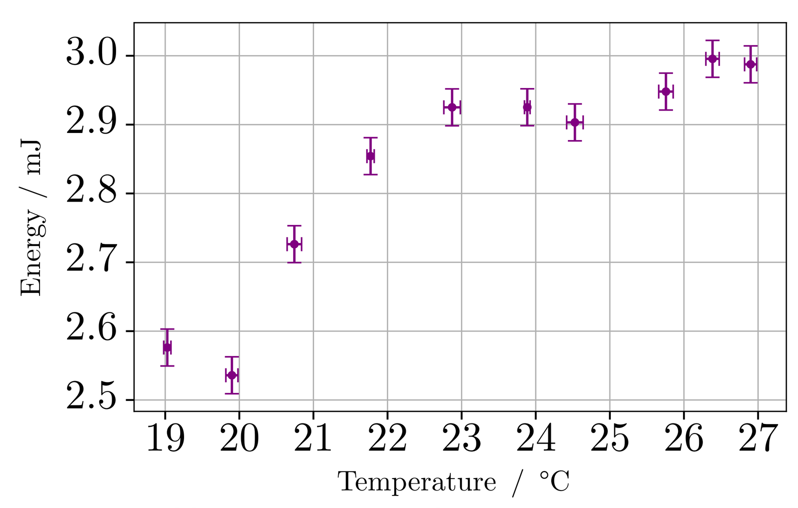

Figure 3: Mean energy output during a temperature scan. The errors in y are the standard deviation in the recorded output energy. The errors in x are the standard deviation of 10 recordings of temperature at each temperature position.

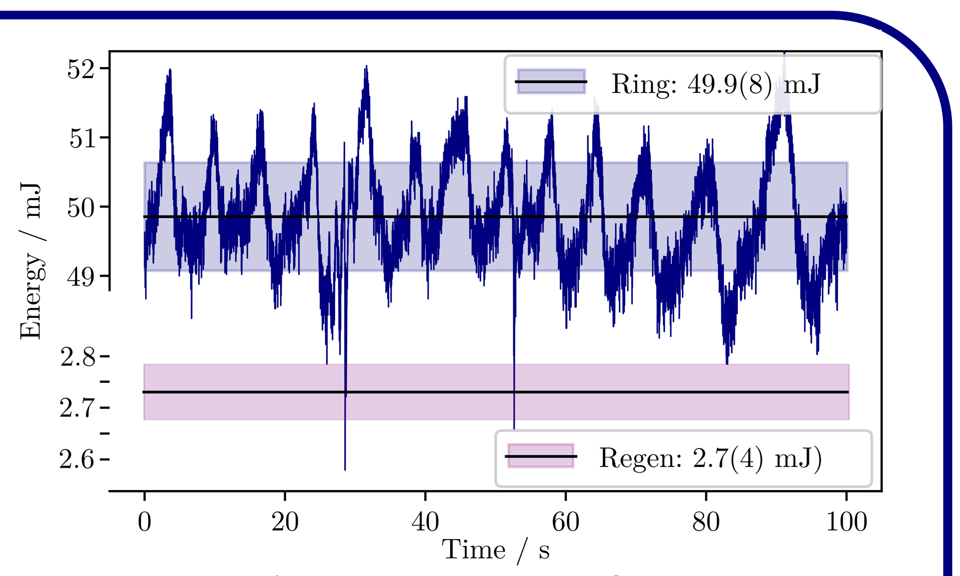

Figure 2: Energy output of both regen and ring amplifiers recorded over 100 s. The shaded regions indicate the standard deviation of the recorded energies.

Despite reaching a saturated energy state, we see a characteristic 'beating' in both amplifiers that is currently unexplained (Figure 2). This relatively long periodicity indicates a thermal rather than optical/electrical effect, however a temperature scan (Figure 3) revealed only the optimum running tempertature. Work to understand this is ongoing.

4. A Future MIR LWFA experiment driven by the Chimera Laser System.

Simulations are currently being undertaken (using the PIC code Smilei) to investigate the pending LWFA experiment driven by the 3.7 µm Chimera laser pulse. We are looking to understand variables over which we have limited control (eg. laser energy and pulse duration), versus variables which we should optimally set (eg. laser waist at focus, acceleration distance and gas density).

The figures show a few examples of the type of analysis being undertaken in order to inform the design of our experiment.

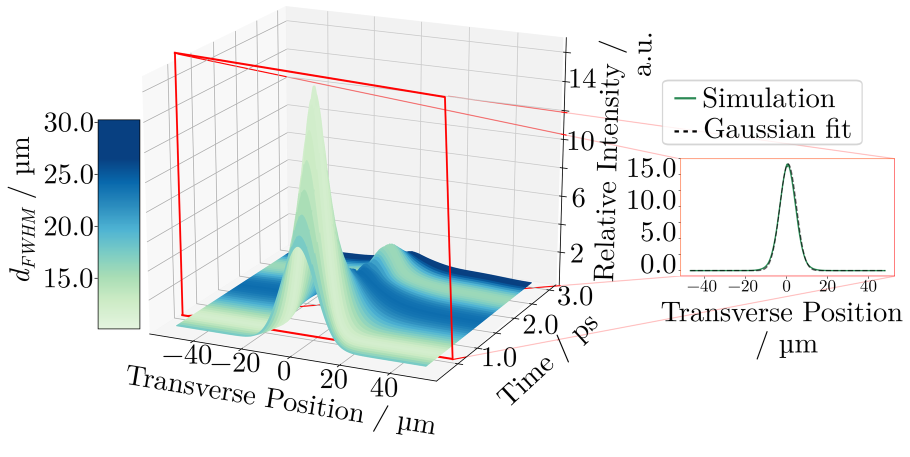

Figure 7: A 3D waterfall plot showing the transverse laser evolution for a LWFA simulation with starting density 2.8 x 10^18 cm^-3. The intensity of the pulses are normalised relative to the highest intensity. The red rectangle highlights the minimum spot size position at 0.55 ps where, using a Gaussian fit, we find the laser to self-focus down to 10.13(1) µm.

[1] N. Thiré et al., Opt. Express 25, 1505-1514 (2017), [2], G. Fan et al., Optica 3, 1308-1311 (2016), [3] M. Bridger et al., Opt. Express 27, 31330-31337 (2019), [4] G. Andriukaitis et. al., Opt. Lett. 36, 2755-2757 (2011)

MURI MIR
MID-INFRARED STRONG-FIELD INTERACTION

ACKNOWLEDGEMENT - This poster presentation has received support from the European Union's Horizon 2020 Research and Innovation programme under Grant Agreement No 101004730 "I.FAST".

EUROPEAN NETWORK FOR NOVEL ACCELERATORS
EuroNNAc4
NPACT supported by EU via I-FAST

I.FAST